

# Spin arrangement diagrams for $\text{Er}_{2-x}\text{R}_x\text{Fe}_{14}\text{B}$ ( $\text{R} = \text{Pr}, \text{Gd}$ )

A. Wojciechowska, A.T. Pędziwiatr\*, B.F. Bogacz, S. Wróbel

*M. Smoluchowski Institute of Physics, Jagiellonian University, Reymonta 4, 30-059 Kraków, Poland*

Received 14 June 2006; received in revised form 10 July 2006; accepted 21 August 2006

Available online 30 January 2007

## Abstract

$^{57}\text{Fe}$  Mössbauer spectroscopy, DSC, X-ray diffraction and magnetic measurements have been applied to study the polycrystalline  $\text{Er}_{2-x}\text{Pr}_x\text{Fe}_{14}\text{B}$  ( $x = 0.25, 0.5, 0.75, 1.0, 1.5$ ) and  $\text{Er}_{2-x}\text{Gd}_x\text{Fe}_{14}\text{B}$  ( $x = 0.5, 1.0, 1.5$ ) compounds. A comparison of results obtained for Pr and Gd-based compounds is presented in this paper.

Special emphasis was put on the spin reorientation phenomena (change of spin orientation from planar to axial arrangement) occurring in these series. The spin reorientation in each compound has been investigated mainly by narrow step temperature scanning in the neighborhood of the spin reorientation temperature,  $T_{\text{SR}}$ .

Initial magnetization versus temperature measurements allowed to establish the temperature regions of reorientations and also the Curie temperatures of the compounds.

The obtained Mössbauer spectra were analyzed by using a procedure of simultaneous fitting and the transmission integral approach. Consistent fits were obtained,  $T_{\text{SR}}$  and the composition dependencies of hyperfine interaction parameters were derived from fits for all studied compounds.

DSC studies proved that the spin reorientations were accompanied by thermal effects. Transformation enthalpy and  $T_{\text{SR}}$  were determined from these studies only for compounds in which  $\text{R} = \text{Gd}$ .

The  $T_{\text{SR}}$  obtained with different methods were analyzed and the spin arrangement diagrams for two series were compared.

© 2007 Elsevier B.V. All rights reserved.

PACS: 76.80.ty; 75.25.tz

Keywords: Intermetallics; Spin reorientation; Magnetic phase diagrams; Mössbauer spectroscopy; Calorimetry

## 1. Introduction

The intermetallic compounds based on  $\text{Er}_2\text{Fe}_{14}\text{B}$  have a tetragonal crystal lattice of the  $\text{P4}_2/\text{mmm}$  space group and belong to the  $\text{Nd}_2\text{Fe}_{14}\text{B}$  structure type, in which there are two non-equivalent positions of Nd ions (4f and 4g), six positions of Fe ions (16k<sub>1</sub>, 16k<sub>2</sub>, 8j<sub>1</sub>, 8j<sub>2</sub>, 4e, 4c) whereas the boron atom is located at one type of site (4g) [1].

From the point of view of fundamental studies, one of the most interesting properties of the Er-based 2:14:1 intermetallic compounds is the spin reorientation occurring in these compounds. In this process, the direction of easy magnetization vector is changing at the reorientation temperature,  $T_{\text{SR}}$ , from planar (in basal plane) to axial (along the *c*-axis) with increasing temperature. It is the result of a competition between axial and

planar tendency in Fe and Er [2,3] sublattice. This phenomenon was studied previously by different groups for Y, Th, Ce, Nd, Ho, Er, Tm [4–14]. The study by single crystal neutron diffraction on  $\text{Er}_2\text{Fe}_{14}\text{B}$  revealed that there is a change of crystal structure to orthorhombic below the spin reorientation transition [12].

The main goal of this work was to compare the effects of competing anisotropies of the two rare earth ions (Er versus Pr and Er versus Gd, suitably) on the spin reorientation phenomena in  $\text{Er}_{2-x}\text{R}_x\text{Fe}_{14}\text{B}$  ( $\text{R} = \text{Pr}, \text{Gd}$ ) using  $^{57}\text{Fe}$  Mössbauer spectroscopy, DSC and magnetic measurements.

## 2. Experimental

The samples of  $\text{Er}_{2-x}\text{Pr}_x\text{Fe}_{14}\text{B}$  and  $\text{Er}_{2-x}\text{Gd}_x\text{Fe}_{14}\text{B}$  were prepared by means of induction melting the stoichiometric proportions of the starting materials in a high purity argon atmosphere followed by annealing at 900 °C for 2 weeks and then rapid cooling to room temperature.

X-ray, thermomagnetic analysis (TMA) and metallographical microscopy indicated the single phase character of the materials. X-ray diffraction analysis was performed at room temperature on randomly oriented powdered samples

\* Corresponding author. Tel.: +48 12 663 55 27; fax: +48 12 663 70 86.  
E-mail address: ufpedziw@if.uj.edu.pl (A.T. Pędziwiatr).

Table 1  
Values of the spin reorientation temperatures for  $\text{Er}_{2-x}\text{Pr}_x\text{Fe}_{14}\text{B}$  and  $\text{Er}_{2-x}\text{Gd}_x\text{Fe}_{14}\text{B}$

Series	$x$	$T_{\text{SRH}}$ [K]	$T_{\text{SRM}}$ [K]	$T_{\text{SRC}}$ [K]	$\Delta H$ [ $\text{J g}^{-1}$ ]	$T_{\text{C}}$ [K]
$\text{Er}_{2-x}\text{Pr}_x\text{Fe}_{14}\text{B}$	0.0 [15]	325	324	–	–	554
	0.25	250	269	–	–	557
	0.5	157	167	–	–	559
	0.75	37	36	–	–	561
	1.0	–	–	–	–	563
	1.5	–	–	–	–	564
	2.0 [17]	–	–	–	–	566
$\text{Er}_{2-x}\text{Gd}_x\text{Fe}_{14}\text{B}$	0.5	303	306	302	0.22	582
	1.0	268	273	270	0.14	603
	1.5	217	220	211	0.08	634

$T_{\text{SRH}}$ , from magnetic measurements;  $T_{\text{SRM}}$ , from Mössbauer studies;  $T_{\text{SRC}}$ , from DSC;  $\Delta H$ , transformation enthalpy;  $T_{\text{C}}$ , Curie temperature;  $T_{\text{SRH}}$  error is  $\pm 2$  K;  $T_{\text{SRM}}$  and  $T_{\text{SRC}}$  error is  $\pm 1$  K;  $\Delta H$  error is  $\pm 0.03 \text{ J g}^{-1}$ ;  $\Delta T_{\text{C}}$  error is  $\pm 1$  K.

with the use of Cr-radiation. TMA was performed by recording magnetization versus temperature,  $M$  versus  $T$ , curves at low external magnetic field with the use of a Faraday-type magnetic balance. The Curie temperatures,  $T_{\text{C}}$ , were also determined from those measurements.

Mössbauer spectra of  $\text{Er}_{2-x}\text{Pr}_x\text{Fe}_{14}\text{B}$  and  $\text{Er}_{2-x}\text{Gd}_x\text{Fe}_{14}\text{B}$  were recorded in the temperature range 18–340 and 80–320 K suitably (with even a 2 K step in the vicinity of  $T_{\text{SR}}$ ) using a  $^{57}\text{Co}$  (Rh) source and a computer driven constant acceleration mode spectrometer. The velocity scale was calibrated by a high purity iron foil. Isomer shifts were established with respect to the centre of gravity of the room temperature iron Mössbauer spectrum.

In case of DSC method, the Gd and Pr-based compounds have been investigated by differential scanning calorimeter Pyris 1. The compounds with gadolinium have been studied in the temperature range 170–370 K and the compounds with praseodymium 100–370 K. The scanning rates were selected from 10 to 60  $\text{K min}^{-1}$  for heating and cooling cycles of measurements.

### 3. Results and discussion

Magnetic measurements enabled the determination of spin reorientation temperature  $T_{\text{SRH}}$  and Curie temperatures  $T_{\text{C}}$  (included in Table 1).

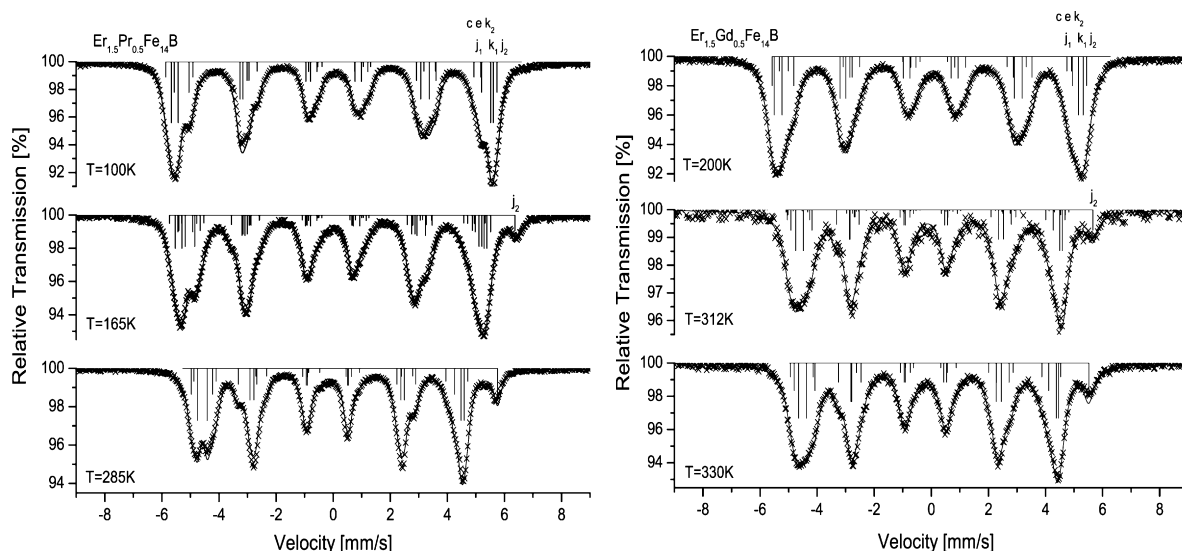


Fig. 1. The examples of experimental  $^{57}\text{Fe}$  Mössbauer spectra of  $\text{Er}_{1.5}\text{Pr}_{0.5}\text{Fe}_{14}\text{B}$  and  $\text{Er}_{1.5}\text{Gd}_{0.5}\text{Fe}_{14}\text{B}$ , intermetallic compounds. The solid lines are fits to the data. The stick diagrams show the line positions and their relative intensities.

A large number of  $^{57}\text{Fe}$  Mössbauer effect spectra for the  $\text{Er}_{2-x}\text{Pr}_x\text{Fe}_{14}\text{B}$  and  $\text{Er}_{2-x}\text{Gd}_x\text{Fe}_{14}\text{B}$  was measured in the regions: below, during and above the transitions. The Mössbauer spectra were analyzed with a transmission integral approach [13]. Each subspectrum was characterised by the three hyperfine interaction parameters: isomer shift—IS, hyperfine magnetic field— $B$ , and quadrupole splitting—QS (defined as  $[(V_6 - V_5) - (V_2 - V_1)]^2$ , where  $V_i$  are velocities corresponding to Mössbauer line positions). One common set of three line widths was used for all Zeeman subspectra. A procedure of simultaneous fitting of several spectra with interconnected parameters was applied in order to get a consistent description of spectra throughout the series, similarly as in our previous studies [11,15,16]. Exemplary spectra for  $\text{Er}_{1.5}\text{Pr}_{0.5}\text{Fe}_{14}\text{B}$  and  $\text{Er}_{1.5}\text{Gd}_{0.5}\text{Fe}_{14}\text{B}$  compounds are presented in Fig. 1. The spectra on the top of figures were recorded in the temperature below the spin reorientation, whereas the bottom of each were obtained above the transition process, the intermediate spectra were measured at temperatures inside the spin reorientation region. The spectra below and above the temperature region of spin reorientation were described using six Zeeman subspectra, called “low” and “high temperature” Zeeman subspectra, respectively, with relative intensities according to iron occupation of the crystallographic sublattices (4:4:2:2:1:1). Inside the temperature region of spin transition, a coexistence of the “low” and the “high temperature” Zeeman subspectra was assumed, which in consequence, gave 12 Zeeman sextets in the spectrum. In the course of transition, the “low” and “high temperature” Zeeman sextets exchange gradually (between themselves) their contributions  $C_1$ ,  $C_h$  to the total spectrum ( $C_1 + C_h = 1$ ). The clear separation of the sixth line of sublattice  $8j_2$  in the “high temperature” spectra (see Fig. 1) makes it easier to estimate those contributions and to determine the spin reorientation temperature from Mössbauer studies,  $T_{\text{SRM}}$ , taken as intersection points of  $C_1$  and  $C_h$  curves [15]. Spin reorientation temperatures obtained by different methods are listed in Table 1.

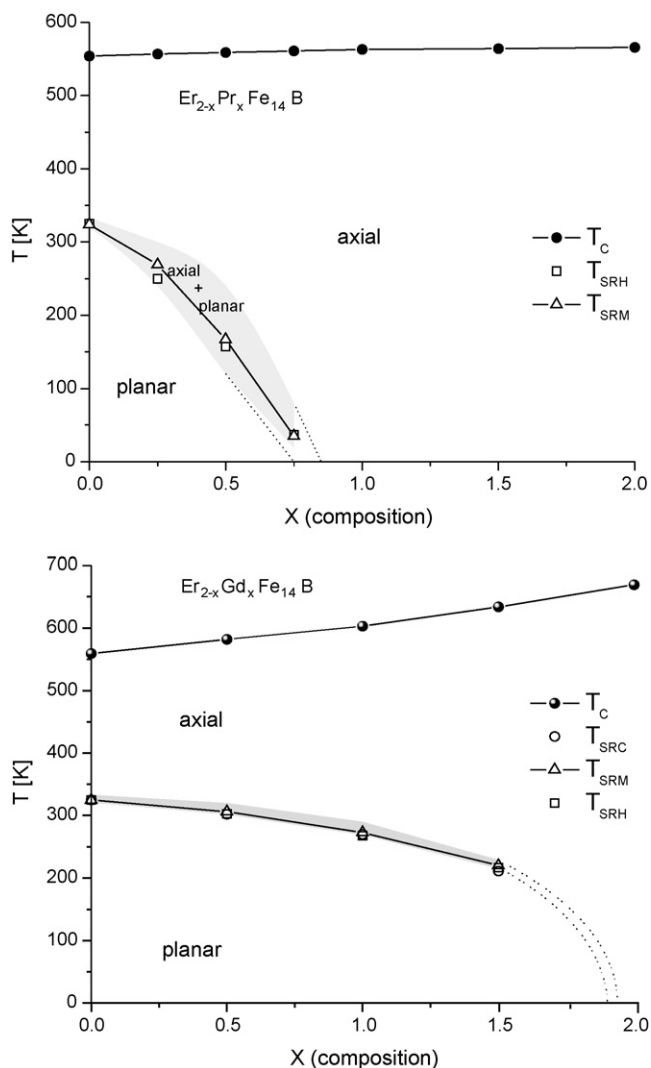


Fig. 2. Spin structure phase diagrams for the  $\text{Er}_{2-x}\text{Pr}_x\text{Fe}_{14}\text{B}$  and  $\text{Er}_{2-x}\text{Gd}_x\text{Fe}_{14}\text{B}$  compounds.  $T_C$ , Curie temperature;  $T_{\text{SRC}}$ ,  $T_{\text{SRM}}$  and  $T_{\text{SRH}}$ , spin reorientation temperatures determined from DSC, Mössbauer and magnetic measurements, respectively. The shaded area marks the coexistence of axial and planar arrangements. Dotted lines mark the probable area of coexistence of planar and axial spin arrangements.

A common linear temperature dependence of IS caused by second-order Doppler shift effect was assumed for “low” and “high temperature” Zeeman sextets for. The systematic changes with temperature of QS (linear) and  $B$  (square polynomial) were taken into account assuming the possibility of a shift of these dependencies between “low” and “high temperature” Zeeman sextets. For all sublattices, the hyperfine field decreases with the increase in temperature and quadrupole splitting is almost independent of temperature, excluding the change of the QS value during the spin reorientation process.

In the DSC calorimetry studies, the endo- and exothermic curves were observed only for the  $\text{Er}_{2-x}\text{Gd}_x\text{Fe}_{14}\text{B}$  compounds. For  $\text{Er}_{2-x}\text{Pr}_x\text{Fe}_{14}\text{B}$  compositions, no conclusive results were obtained. The endothermic peaks correspond to the transition from basal to axial easy magnetization direction on increasing temperature. The spin reorientation temperatures derived from this method,  $T_{\text{SRC}}$ , were taken as the arithmetic average of temperatures obtained for heating and cooling cycles. The area under the DSC peak is defined as the transformation enthalpy,  $\Delta H$ . It was obtained as the arithmetic average of enthalpies for the cooling and heating cycles (Table 1).

Fig. 2 shows the magnetic phase diagrams for the studied systems. For each composition, the axial spin arrangement dominates at high temperatures while planar arrangement is possible at lower temperature. It is visible that the substitution of Pr and Gd for Er causes the decrease of the spin reorientation temperature and the reduction of planar anisotropy range. This process is much stronger for Pr- than for Gd-substitution. Additionally, for Pr-substituted compounds, the ranges of transitions from planar to axial arrangements are larger than in case of Gd-substituted compounds (it is visible on Fig. 2 as a grey area—region of coexistence of axial and planar arrangements).

## References

- [1] J.F. Herbst, J.J. Croat, F.E. Pinkerton, W.B. Yelon, *Phys. Rev. B* 29 (1984) 4176–4178.
- [2] D. Givord, H.S. Li, R. Perrier de la Bâthie, *Solid State Commun.* 51 (1984) 857–860.
- [3] S. Hirose, Y. Matsuura, H. Yamamoto, S. Fujimura, M. Sagawa, H. Yamauchi, *J. Appl. Phys.* 59 (1986) 873–879.
- [4] E. Burzo, *Rep. Prog. Phys.* 61 (1998) 1099–1266.
- [5] K.H.J. Buschow, in: E.P. Wohlfarth, K.H.J. Buschow (Eds.), *Ferromagnetic Materials*, vol. 4, Elsevier, Amsterdam, 1988, pp. 1–129.
- [6] K.H.J. Buschow, *Rep. Prog. Phys.* 54 (1991) 1123–1213.
- [7] M.R. Ibarra, Z. Arnold, P.A. Algarabel, L. Morellon, J. Kamarad, *J. Phys. Condens. Matter.* 4 (1992) 9721–9734.
- [8] A.T. Pędziwiatr, W.E. Wallace, *J. Less-Common Met.* 126 (1986) 41–51.
- [9] C. Piqué, R. Burriel, J. Bartolomé, *J. Magn. Magn. Mater.* 154 (1996) 71–82.
- [10] N.C. Koon, B.N. Das, C.M. Williams, *J. Magn. Magn. Mater.* 523 (1986) 54–57.
- [11] A.T. Pędziwiatr, B.F. Bogacz, A. Wojciechowska, S. Wróbel, *J. Phys. Condens. Matter.* 17 (2005) 6999–7008.
- [12] P. Wolfers, M. Bacmann, D. Fruchart, *J. Alloys Compd.* 317–318 (2001) 39–43.
- [13] B.F. Bogacz, *Mol. Phys. Rep.* 30 (2000) 15–20.
- [14] E.B. Boltich, A.T. Pędziwiatr, W.E. Wallace, *J. Magn. Magn. Mater.* 66 (1987) 317–322.
- [15] R. Wielgosz, A.T. Pędziwiatr, B.F. Bogacz, S. Wróbel, *Mol. Phys. Rep.* 30 (2000) 167–173.
- [16] A.T. Pędziwiatr, B.F. Bogacz, A. Wojciechowska, *J. Alloys Compd.* 396 (2005) 54–58.
- [17] A.T. Pędziwiatr, S.G. Sankar, W.E. Wallace, *J. Appl. Phys.* 63 (1988) 3710.